Advances in Aircraft and Spacecraft Science, *Vol. 7, No. 6 (2020) 475-493*
DOI: https://doi.org/10.12989/aas.2020.7.6.475

Characterization of the mechanical behavior of PEKK polymer and C/PEKK composite materials for aeronautical applications below and above the glass transition temperature

Giuseppe Pedoto[1a], Olga Smerdova[1b], Jean-Claude Grandidier[1c], Marco Gigliotti*[1] and Alain Vinet[2d]

[1]Department of Physics and Mechanics of Materials, PPRIME Institute, CNRS, ISAE-ENSMA, University of Poitiers, France
[2]Airbus S.A.S. 2, Building D42 18 Marius Terce 31025 Toulouse France

(Received October 14, 2019, Revised May 5, 2020, Accepted May 8, 2020)

Abstract. This paper is focused on the characterization of the thermomechanical properties of semicrystalline poly-ether-ether-ketone (PEKK) and of carbon fiber reinforced thermoplastic based laminated composites (C/PEKK) below and above the glass transition temperature (T_g). Differential Scanning Calorimetry (DSC), Dynamic Mechanical Analysis (DMA) and tensile tests are carried out on both pure PEKK polymer and $[(\pm45)_2, +45]_s$ C/PEKK composite samples, showing a significant similarity in behavior. The employment of a simple micromechanical model confirms that the mechanical and physical behavior of the polymer and that of the matrix in the composite are similar.

Keywords: PEKK; carbon fiber reinforced thermoplastic matrix

1. Introduction

In the past 60 years, the aeronautic industry has progressively replaced a larger percentage of metal components with carbon fiber reinforced polymers, aiming for mass and cost reduction of aircraft structures. Furthermore, in the last 30 years, different studies have been carried out to replace the thermoset polymers employed as composites' matrices with thermoplastic polymers, to increase the maximum operational temperatures and because of the possibility to be recycled, (Biron 2018, Gabrion *et al.* 2016, Martín *et al.* 2017, Tadini *et al.* 2017, Pappadà *et al.* 2015).

The PEKK is a semicrystalline polymer of the PAEK family, with properties similar to the more used PEEK. It has been shown that the presence of the crystalline phase for PEEK (Martineau *et al.* 2016) reduces the properties loss registered in almost amorphous PEEK if the temperature is raised above the glass transition temperature (T_g). Other studies, carried out on the PEEK below its

*Corresponding author, Professor., E-mail: marco.gigliotti@ensma.fr
[a]Ph.D. Student, E-mail: giuseppe.pedoto@ensma.fr
[b]Associate Professor, E-mail: olga.smardova@ensma.fr
[c]Professor, Email: jean-claude.grandidier@ensma.fr
[d]Ph.D., E-mail: alain.vinet@airbus.com

http://www.techno-press.org/?journal=aas&subpage=7 ISSN: 2287-528X (Print), 2287-5271 (Online)

T_g, have shown the presence of physical ageing and the possibility of correcting the William – Landel - Ferry (WLF) law to obtain a time-temperature superposition (Brinson and Gates 1995, Guo and Bradshaw 2007). Some studies on C/PEKK composites (Choupin *et al.* 2017, Chelagma *et al.* 2017) have shown that the presence of the fibers may change the crystallization kinetics, in addition to the constraints applied to the matrix by the fiber themselves, leading to question if the behavior of the matrix inside the composite is similar to that of the pure polymer. To the author's knowledge, there is no established literature about the PEEK thermomechanical behavior for temperatures above the glass transition temperature and for a wide temperature spectrum.

Several studies on the PEKK polymer have described the crystallization kinetics (Choupin *et al.* 2017, Li *et al.* 2019) and showed the impact of the crystalline phase percentage, produced during the manufacturing process, on the mechanical properties below and above T_g (T_g = 160°C) (Choupin *et al.* 2017). The presence of chemical phenomena at temperatures higher than T_g has been shown, and particularly in a temperature range between 250°C and T_m = 330°C, where the material degrades because of oxidation and morphological changes (Vinet *et al.* 2019). Consequently, 250°C can be considered as a limit for using these composites. The elastic-plastic behavior LDF^{TM} AS-4/PEKK composite system below and above T_g was studied in Sun et al 1992, leading to some quantitative information about the existence of a plastic phase and failure strength during composite monotonous traction.

This study aims at characterizing the mechanical behavior of PEKK polymer and C/PEKK composite materials in a wide temperature range below and above T_g, particularly in a temperature range between 160°C and 200°C, where the effect of physical ageing is not expected, and oxidation phenomena should be negligible. The presence of the crystalline phase in PEKK is expected to reduce the properties loss observed when raising the temperature above T_g, due to the effect of the amorphous phase, as observed for PEEK polymers (Martineau *et al.* 2016).

2. Material, experimental setup and methods

2.1 Materials

As shown by Choupin (2017), at 180°C, the properties of PEKK increase with the crystalline phase, therefore this study is focused on the highest properties configuration of both polymer and composite.

The materials tested in this study are: the semicrystalline (SC) PEKK 7002 (nominal 24% of crystalline phase, maximum achievable during cooling process), manufactured by Arkema, and the [(±45)2, +45]s composite, manufactured by Airbus SAS from prepregs of SC PEKK 7002 and AS4C carbon fibers, with a strong crystalline phase (nominal 28% of crystalline phase, maximum achievable during the cooling process). The properties of the SC PEKK are listed in Table 1. The

Table 1 PEKK 7002 properties

Property	Value
Glass transition temperature - T_g	160°C
Melting temperature – Tm	330°C
Crystalline phase % - χ	24% (max)

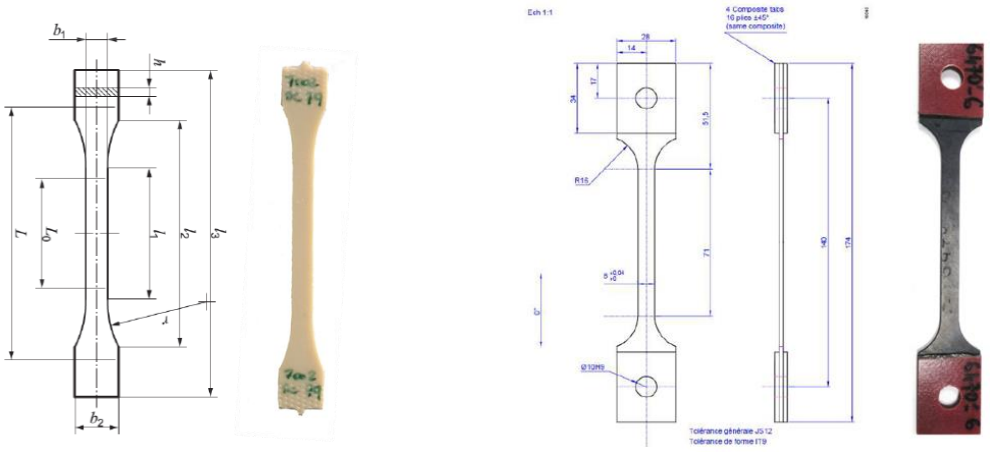

(a) PEKK specimens (b) C/PEKK specimens

Fig. 1 Geometry of the tensile tests samples

specimens employed for the tensile tests on PEKK and C/PEKK are showed in Fig. 1.

2.2 Methods

The methods described below refers to the experimental campaign carried out on both PEKK and C/PEKK samples, which results are showed in Section 3.

2.2.1 Tensile tests

Tensile tests were carried out on an Instron 4505 servo-hydraulic machine, which has loading cell capacity of 0.5/2/5/50/100 KN and a max displacement speed of 500 mm/min. In order to carry out tests at temperatures higher than room temperature, the machine was equipped with a regulated oven. This allows to reach temperatures from -100°C up to 200°C. The Videotraction system was employed for strain measurement and its further discuss in Section 2.3. All tests on both PEKK and C/PEKK composite samples were carried out at different temperatures from room temperature to 200°C, on dogbone specimens showed in Fig.1, at different constant displacement rate of 0.1, 1 and 10 mm/min, employing a of 2000 N loading cell. Each tensile test at temperature higher than room temperature preceded by a heating phase, needed for allowing the hoven to reach the thermal equilibrium at the testing temperature. During this preliminary phase the test was force driven at 0.3 N for 41 min (≈ 2500 s), time needed to reach a stabilized value of 200°C.

2.2.2 Indentation tests

Local elastic and plastic properties of PEKK polymer were measured by nanoindentation technique at different temperatures. These tests were carried out on NanoTest Vantage nanoindenter supplied by Micro Materials Ltd. It is a force-controlled vertical pendulum system with electromagnetic force actuator and capacitive depth measurements. The load range available with Low Load head is up to 500 mN with load resolution of 2 nN and maximal indentation depth of 20 μm with the noise floor of 0.3 nm. The high temperature module consist of two separate heating systems with temperature control for the indenter and the sample. The sample is cemented

on the sample holder with Omega Bond 600 cement which conduct high temperatures and does not degrade during the testing. All room and high temperature tests were performed with the same indenter diamond spherical tip. The nominal radius of indenter tip was 25 μm. The area function was determined with fused silica to represent more accurately the results at low depths.

A PEKK tensile sample was cut into small square pieces with a side of 5mm and polished thoroughly until roughness of several nanometers was achieved. The nanoindentation tests were carried out at 10 mN load at a constant loading/unloading rate of 0.5mN/s. The temperature during testing at room temperatures was around 24°C. At high temperatures, tests were carried out at 150°C, 165°C, 180°C and 200°C, immediately after heating. The load-displacement curves were analyzed by Oliver&Pharr method (Oliver *et al.* 1992) to obtain the elastic indentation modulus (EIT), which is usually compared to Young's modulus for elasto-plastic materials, and the Hardness (H), which describes plastic behaviour.

2.2.3 DMA tests

All the Dynamical Mechanical Analysis (DMA) tests were carried out on a TA Instrument DMA Q800, which has a temperature range of -150 to 600°C, an applicable force range of 0.0001 to 18 N, a frequency range of 0.001 to 200Hz, a heating rate range of 0.1 to 20°C/min and a cooling rate range of 0.1 to 10°C/min. Different sets of grips allow to carrying out tensile, single cantilever, 3 point bending and shear DMA test.

3-point-bending DMA tests were carried out on both 70x10x2.11 mm PEKK and C/PEKK specimens, varying the temperature from 20°C to 200°C, at 2°C/min heating rate, at 1 Hz, imposing an amplitude of displacement of 15μm.

2.2.4 DSC tests

All the Differential scanning calorimetry (DSC) tests were carried out on a TA Instrument DSC Q20, which has a temperature range (thanks to the employing of a refrigerated cooling system TA Instrument RCS 90 with the employment of liquid nitrogen) of -90 to 550°C, standard or modulated analysis and its provided with the Tzero technology.

Some samples were cut from the as-received SC PEKK and others from the previously tested specimens. Those samples were tested with DSC, varying the temperature from 20°C to 360°C, keeping the temperature constant from 5 min (preventing the material degradation), then they were cooled to 20°C and re-heated up to 360°C; all the heating and cooling ramps were carried out at 10°C/min. DSC tests on the as-received C/PEKK were also carried out.

2.3 Displacement, strain and stress measurement system

The carrying out of the experimental campaign required the possibility of measuring stress and strain at relatively high temperature (up to 200°C) and in real time. Thus, at first, the Videotraction System, was employed during all the tensile and tests. It employs a video camera, which records the gauge length of the specimen were 4 markers are painted. Through the IdPix software (developed at the ISAE-ENSMA, Poitiers), the system evaluates their centers of mass and, measuring the variation of the distance between the vertical and horizontal couples and exploiting finite difference method, it is capable to measure the true strains and true stresses in real time. Furthermore, it requires a low definition camera only, implying low data volume. However, the downside of this technique is that the combination of relatively high temperatures and the large measured strains, may produce a degradation of the marker's paint.

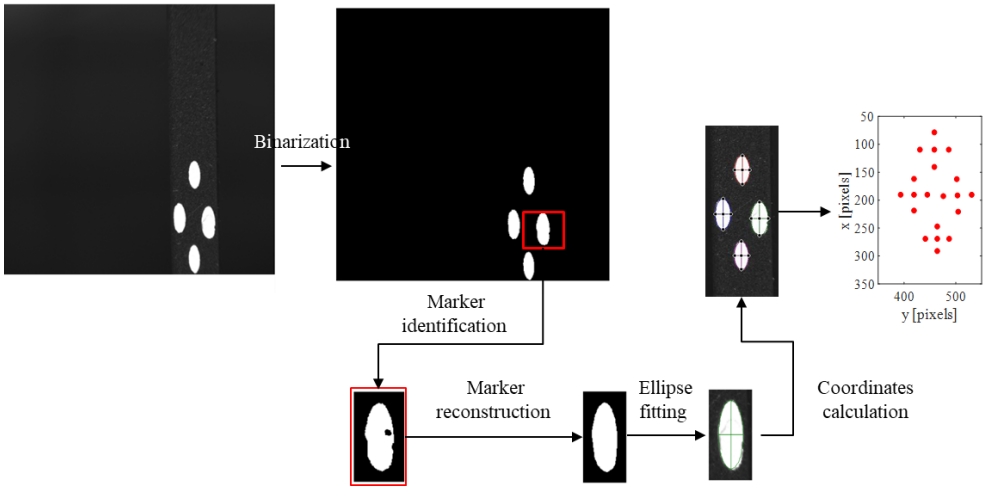

Fig. 2 Image analysis algorithm by IAT

The IdPix performance can be tested by employing Digital Image Correlation (DIC). This technique requires a pattern instead of markers and a richer greyscale histogram (compared to the almost binarized images taken for VT), forcing the repetition of the whole test campaign. To reduce errors a higher definition camera is needed, which increases more than ten times the data volume size. Moreover, it employs a searching windows that need a predictive formulation to estimate the subsequent position of the searching window itself (Sutton *et al.* 2010) and it results with the fact that it could not be able to follow the whole test duration, precisely because of the large measured strains. More importantly, also the pattern could be affected by the same degradation saw on the markers, in fact not solving the weakness of VT.

For those reasons, the DIC was not used in the analysis and a post-test measurement system was developed, the Image Analysis Tool (IAT). The IAT is able to work on the same images acquired during the tests to employ the Videotraction system. Contrary to DIC, the IAT does not requires a mobile searching window, because it researches the marker in the whole image or in a fixed subset of it: this analysis is still faster than DIC analysis, because of the lower images size acquired for VT.

Moreover, the IAT capable to automatically restore the degraded markers, filling the internal holes and reconstructing the holes on the marker perimeter with a convex hull. The reconstructed edge of each marker is then fitted with an ellipse: this allows to obtain 5 points (major and minor axis ends and their intercept) or more for each marker, instead of just one. An example of the whole proceeding is shown in Fig. 2.

The coordinates of those 20 points are then compared to a reference image (varying consequently to the formulation employed) to calculate the displacement fields in the longitudinal and transversal direction.

Employing the finite difference, it is possible to evaluate the true strains (and then the engineering strains), but for each couple combination of the 20 points instead than just for the vertical and horizontal couples of centers of mass, as it is done by VT software IdPix.

Moreover, the IAT does not require a predictive function for establish the subsequent position of the searching window (needed for the DIC analysis) simply because of the absence of the searching window itself.

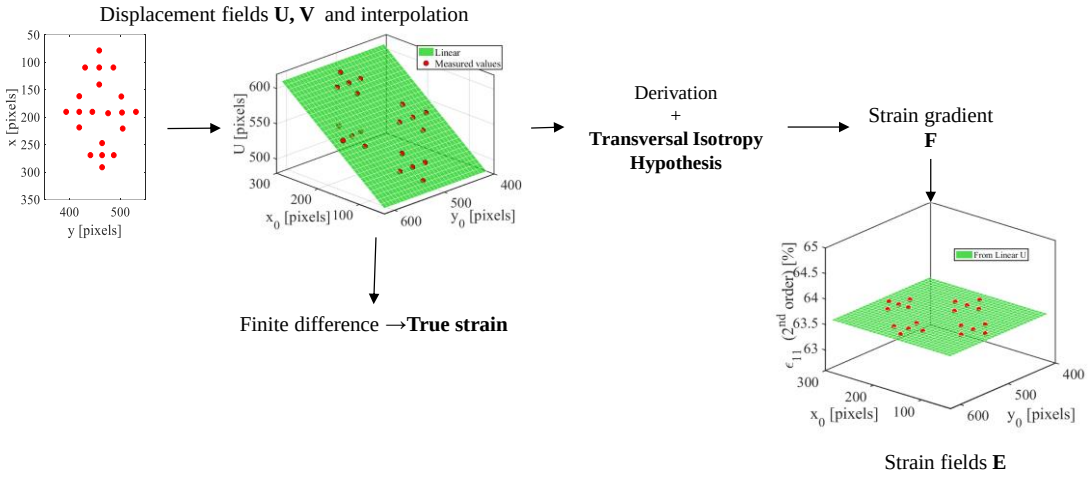

Fig. 3 Strains calculation algorithm of IAT

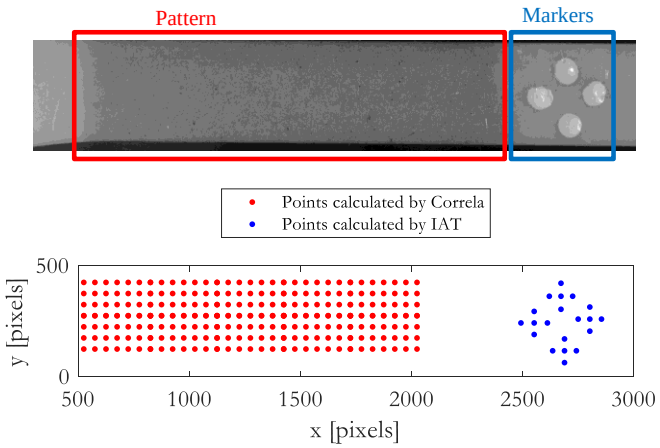

Fig. 4 Specimen employed for IAT validation: in red the pattern and in blue the markers and the coordinates of the points identified by DIC and IAT respectively

In order to describe the strain fields with higher order formulations, two bilinear polynomial functions are employed to fit the displacement fields in longitudinal and transversal directions after measurement (Fig. 3). The displacement functions are then derived, and under the transversal isotropy hypothesis, the strain gradient ***F*** is calculated. This allows to evaluate the 3D strain fields (Fig. 3) to calculate the strains fields. Different formulations are implemented in the IAT: Total and Update Lagrangian, Eulerian (Gurtin *et al.* 2010), Logarithmic and Engineering formulations. 3D strains could be deduced under the hypothesis of transverse isotropy.

The IAT was validated through comparison with DIC software Correla, analyzing the images taken during a tensile test at 200°C and 1 mm/min, were both Videotraction markers and DIC pattern were painted on the specimen gauge length. Fig. 4 shows the initial points evaluated by both Correla and IAT.

The comparison of the strains measured by IAT and DIC (Fig. 5) showed an almost perfect

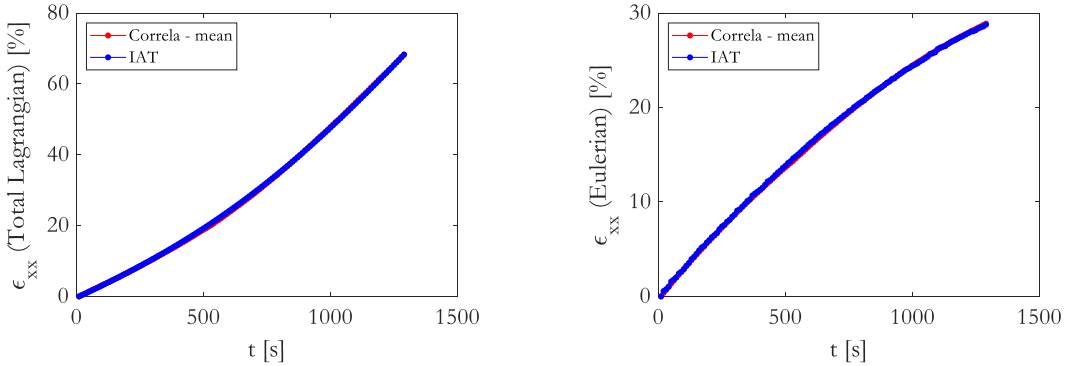

(a) Total Lagrangian formulation (b) Eulerian formulation

Fig. 5 Comparison between IAT and DIC results

superposition, validating the IAT, for both Total Lagrangian and Eulerian formulation.

The IAT is able to work in post-treatment only: it is therefore complementary to the VT system and able to prevent or at least reduce the data loss, without changing at all the data size. The combination of VT and IAT gave us a robust measurement system which has been employed for tensile and creep tests.

3. Results and discussion

3.1 Characterization of the thermo-mechanical behavior of PEKK polymer

3.1.1 Tensile tests

Tensile tests were carried out at different temperatures from room temperature to 200°C, at 1 mm/min, and the results are shown in Fig. 6: there is a decreasing of the apparent stiffness and the maximum stress and an increasing of the ductility and strain at rupture as the temperature increases. Furthermore, while under T_g, a localized and sharp necking appears, and the more the temperature is increased, the more it extends along the gauge lengths before failure. Its appearance is signaled by a peak in the force-position curve, as showed in Fig. 6. However, as the temperature is increased over T_g, the necking is more diffused along the overall gauge length and more gradual; as consequence no peak appears in the force vs position curve.

Images were acquired during the heating phase and analyzed with the IAT, allowing to follow the volumetric changes along with the temperature increasing, showed in Fig. 7. Once the temperature is increased over T_g, a change of slope appears in the curves, proving the presence of physical ageing seen in the PEEK.

Other tensile tests were carried out at 3 temperatures above T_g (165°C, 180°C and 200°C) at different displacement speeds (0.1, 1 and 10 mm/min) to investigate time effect (Fig. 8). No pure elastic region is clearly identifiable at any condition of temperature and speed. When the temperature is close to around T_g (at 165°C= T_g +5°C), the increase of displacement speed produces an increase of the apparent stiffness. Instead, moving at higher temperatures, the material seems less sensitive to temperature and time effects.

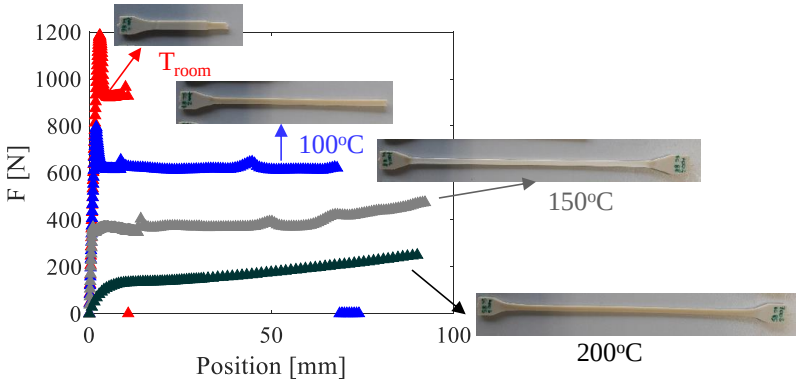

Fig. 6 Force vs position curves obtained from tensile test on SC PEKK from room temperature to 200°C at 1 mm/min

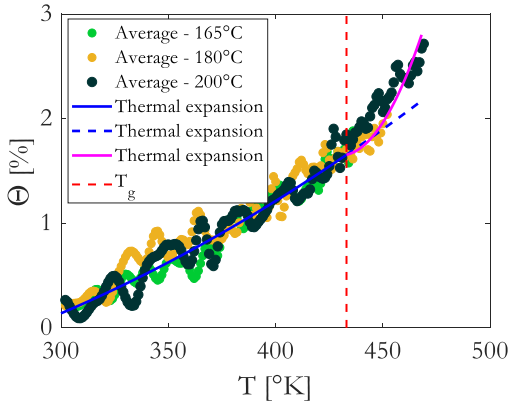

Fig. 7 Volumetric changes vs temperature obtained from heating phase before tensile tests at temperature higher than room temperature

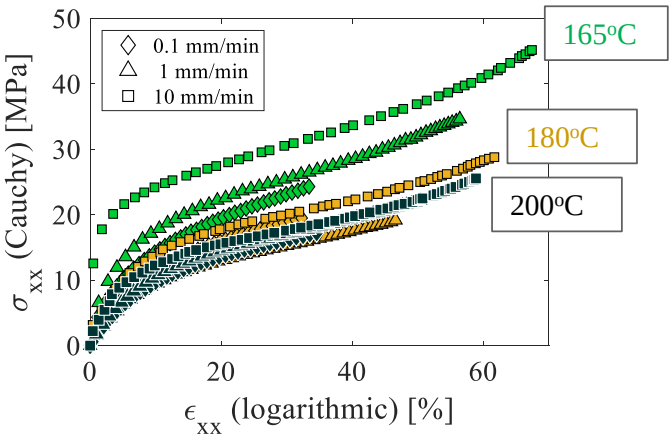

Fig. 8 Stress vs strain curves obtained from tensile test on SC PEKK and at 165°C, 180°C and 200°C at 0.1 mm/min, 1 mm/min and 10 mm/min

Table 2 Initial tensile moduli obtained from tensile test on SC PEKK and from room temperature to 200°C at 1 mm/min

$\dot{z}$ [mm/min]	T [°C]	Initial tensile modulus [MPa]
1	20	3793
	100	3750
	150	3126
	165	543
	180	171
	200	178

The initial tensile modulus was evaluated at each temperature through a linear regression between 0.1% and 0.4% true strain. In Table 2 the values corresponding to all tensile tests at a speed of 1 mm/min are resumed.

3.1.2 Indentation tests

Indentation tests (Fig. 9) were carried out at the same 3 temperatures, others than room temperature and 150°C, and allowed to measure the indentation moduli (with a Poisson's ratio of 0.4), which are resumed in Table 3.

3.1.3 DMA tests

3-point-bending DMA show a severe decrease of the storage modulus (around 90%) as the temperature is increased above T_g.

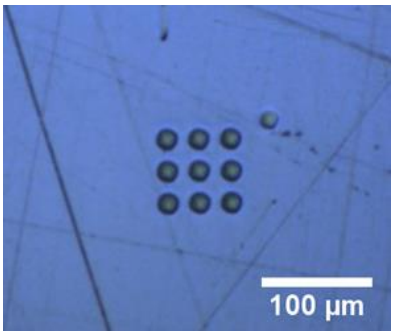

Fig. 9 Indentation marks on SC PEKK

Table 3 Indentation moduli obtained from indentation test on SC PEKK from room temperature to 200°C

T [°C]	Elastic Indentation modulus [MPa]
20	4560
150	3710
165	1280
180	150
200	120

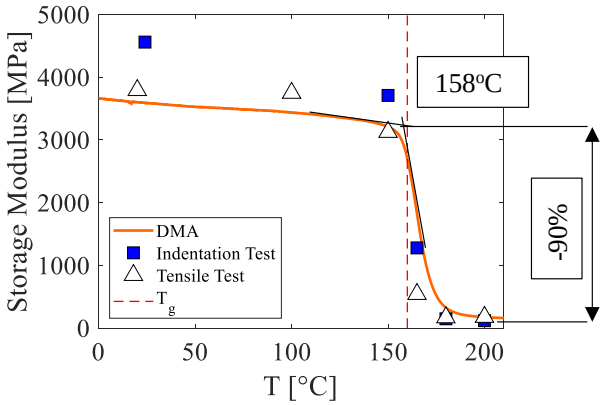

Fig. 10 DMA storage modulus between 20°C and 200°C, compared with initial tensile moduli and indentation moduli

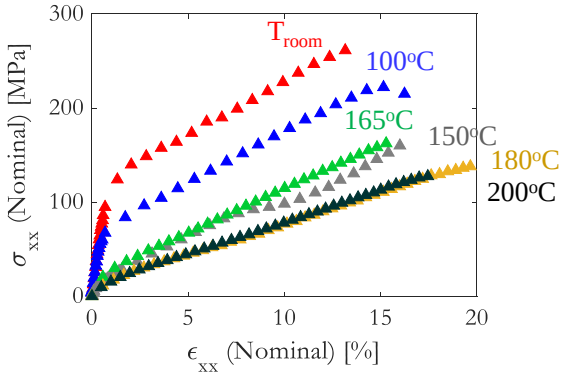

Fig. 11 Nominal stress vs nominal strain obtained from tensile tests on C/PEKK from room temperature to 200°C at 1 mm/min

Fig. 10 shows also the comparison with initial tensile moduli and indentation moduli: the properties loss of the storage modulus is confirmed by both the tensile and indentation moduli. Moreover the storage modulus trend confirms the lower sensibility to temperature effects at 180°C and 200°C, compared to 165°C, because the PEKK, at this latter temperature, is still in the transition region, while at higher temperature it reaches a more stable region.

3.2 Characterization of the thermo-mechanical behavior of C/PEKK composites

An analogous experimental campaign was carried out on $[(\pm 45)_2, +45]_s$ composite specimens, to characterize the C/PEKK mechanical and physical-chemical behavior. The choice of orientation was made in such a way as to highlight the influence of the matrix on the composite behavior.

3.2.1 Tensile tests

Tensile tests were carried out at different temperatures from room temperature to 200°C and at 1 mm/min, also on C/PEKK specimens, and the results are shown in Fig. 11: there is a decreasing of the apparent stiffness and the maximum stress and an increasing of the ductility and strain at rupture as the temperature increases, similarly to what observed on the pure polymer.

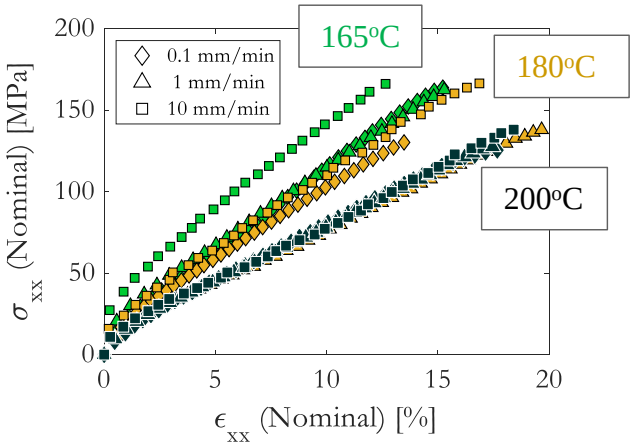

Fig. 12 Nominal stress vs nominal strain obtained from tensile tests on C/PEKK at 165℃, 180℃ and 200℃ at 0.1 mm/min, 1 mm/min and 10 mm/min

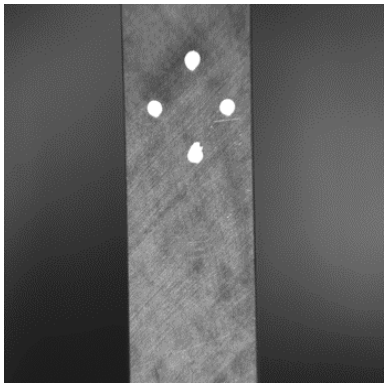

(a) C/PEKK specimen's surface

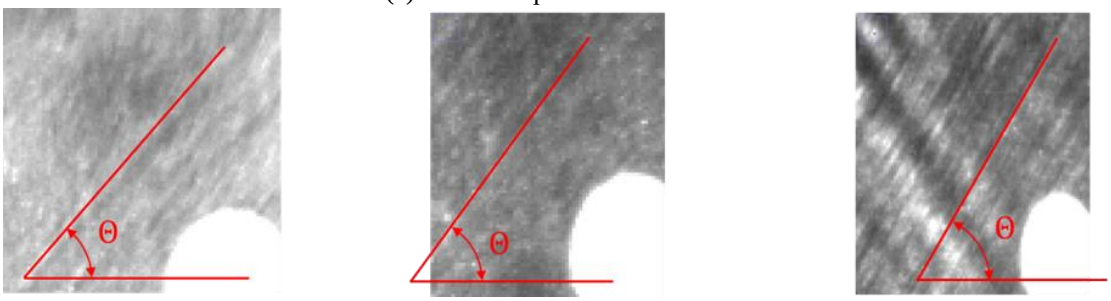

(b) Fiber rotation at different times during tensile test

Fig. 13 Composite specimen surface, (a) and fiber rotation during the tensile test, (b)

Tensile tests were carried out at the same 3 temperatures above T_g and 3 displacement speeds applied to the SC PEKK (see 3.1): the results are showed in Fig. 12.

Fiber orientation is clearly identifiable on the surface of the specimens (Fig. 13) and therefore it is possible to measure it during tests, showing up to 15° fiber rotation during tensile tests, which have a linear dependency on the strain and a quadratic dependency on stress (Fig. 14).

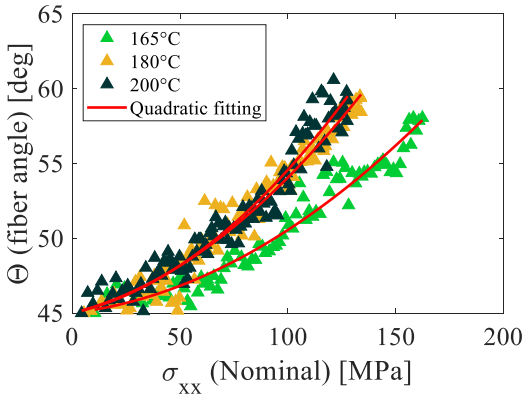

Fig. 14 Fiber orientation vs nominal stress measured during tensile tests at 165°C, 180°C, 200°C

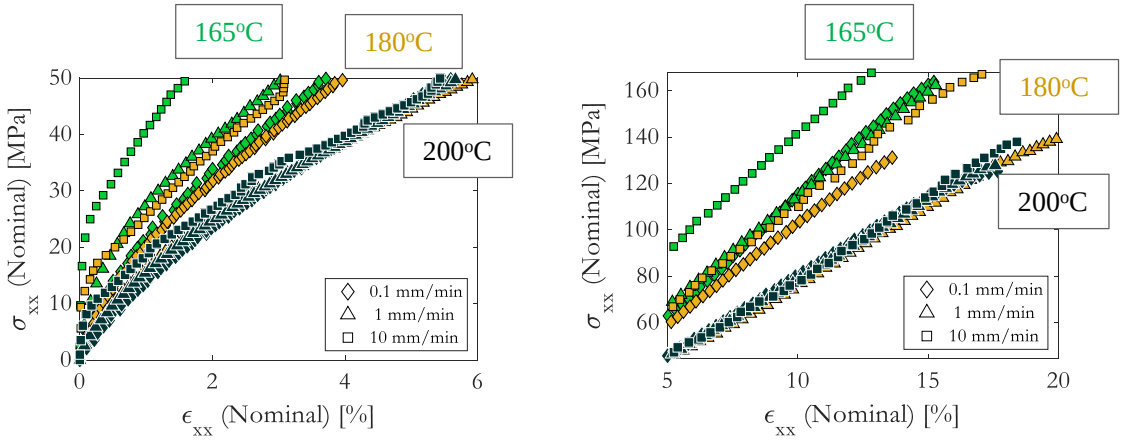

(a) Matrix dominated region at low strains (b) Fiber dominated region at high strains

Fig 15 C/PEKK tensile tests nominal stress vs nominal strain curves

Table 4 Initial tensile moduli obtained from tensile test on C/PEKK and from room temperature to 200°C at 1 mm/min

$\dot{z}$ [mm/min]	T [°C]	Initial tensile modulus [MPa]
1	20	16558
	100	14436
	150	7090
	165	2425
	180	1868
	200	1795

Looking at the stress vs strain curves of the C/PEKK, the low strain region shows temperature and time effects similar to the ones described for SC PEKK, suggesting not only that there could be a similarity in behavior between the matrix and the polymer, but also that the composite behavior is matrix dominated at low strains (Fig. 15(a)). Moreover, at higher strains, there is a

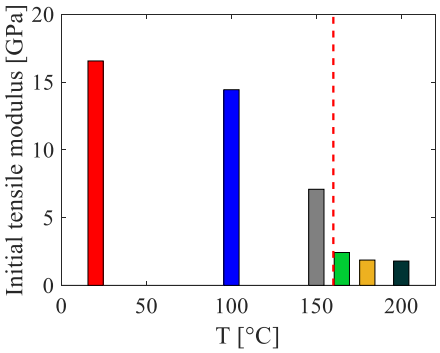

Fig. 16 Initial tensile moduli obtained from tensile test on C/PEKK and from room temperature to 200℃ at 1 mm/min

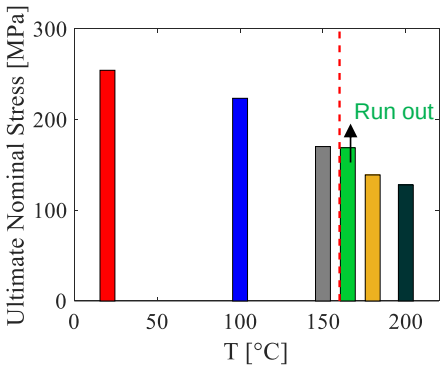

Fig. 17 Ultimate nominal stress obtained from tensile test on C/PEKK and from room temperature to 200℃ at 1 mm/min

Table 5 Ultimate nominal stress obtained from tensile test on C/PEKK and from room temperature to 200°C at 1 mm/min

$\dot{z}$ [mm/min]	T [℃]	Ultimate Nominal Stress [MPa]
1	20	254.4
	100	223.5
	150	170.6
	165	>169
	180	139
	200	128

more linear behavior of nominal stress as function of nominal strain, which suggests the presence of a fiber dominated region (Fig. 15(b)).

The C/PEKK tensile modulus, calculated through a linear regression between 0.01% and 0.3% nominal strain. In Table 4 the values corresponding to all tensile tests at a speed of 1 mm/min are resumed.

The C/PEKK ultimate nominal stresses obtained from 1 mm/min tensile tests are listed in Table 5. In order to apply always the same test protocol to the C/PEKK, all the C/PEKK specimens were

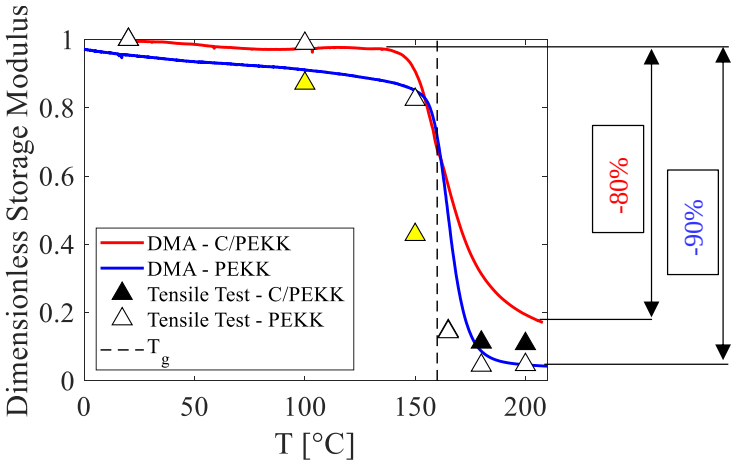

Fig. 18 Dimensionless storage modulus and initial tensile modulus of PEKK and C/PEKK

tested with a 2000 N load cell: this prevented to reach the failure of the specimen at 165°C, because the required force value exceeded the load cell capacity. In Table 5 the last measured value is reported, which is also employed for Fig. 17 to show its order of magnitude comparing to other temperatures.

3.2.2 DMA tests

DMA tests on the C/PEKK and, together with the initial tensile moduli, compared to the polymer storage modulus and tensile moduli.

To simplify the comparison, all moduli were normalized respect to their initial values and the results are showed in Fig. 18. The loss of properties is anticipated in the C/PEKK (lower T_g onset) and it is lower (80%) compared to the PEKK. However, there is a global similarity between polymer and composite behavior.

3.3 Physical-chemical characterization of PEKK polymer and C/PEKK composites before and after thermo-mechanical tests

3.3.1 DSC

DSC tests on as-received and mechanically tested SC PEKK allowed measuring the 1st heating heat flow vs temperature curves (Fig. 19(a)) which show no exothermic peak between the inflection point (corresponding to the T_g) and the endothermic peak (corresponding to the melting point): this absence implies that no cold crystallization happens, or that there is no increase in crystallinity percentage produced only by thermal loads.

Comparing the inflection points, there are negligible difference in the T_g measured values, before and after mechanical tests. The area of the endothermic peak gives the enthalpy of transition related to the melting of the crystalline phase and allows to evaluate the amount of crystalline percentage in the sample, trough the equation:

$$\chi = \frac{\Delta H_{melt} - \Delta H_{cold\ cryst}}{\Delta H_{100}} = \frac{Area_{peak}}{\dot{T}\ \Delta H_{100}} \tag{1}$$

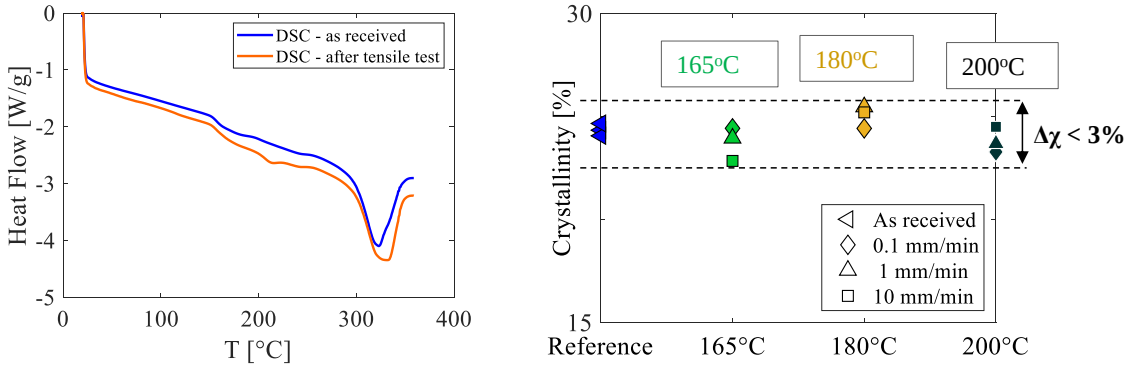

(a) Heat flow vs T curves (b) Crystalline percentages

Fig 19 Comparison between before and after tensile test

Table 6 Ultimate nominal stress obtained from tensile test on C/PEKK and from room temperature to 200°C at 1 mm/min

As received	24.34
	24.06
	24.66

After tensile test		
T [°C]	$\dot{z}$ [mm/min]	Crystalline percentages [MPa]
165	0.1	24.43
	1	23.95
	10	22.84
180	0.1	24.42
	1	25.47
	10	25.05
200	0.1	23.28
	1	23.68
	10	24.50

where $\dot{T}$ is the heating rate, and ΔH_{100} =130 J/g is the theoretic endothermic enthalpy for 100% crystalline phase.

As shown in Fig. 19(b), all the measured values of crystalline percentage, obtained from DSC before and after testing, are in a range of 3% of crystallinity and they are resumed in Table 6. This leads to conclude that no crystallinity percentage changes takes place because of tensile thermal-mechanical loading on SC PEKK.

DSC tests on the as-received C/PEKK were also carried out. Because of the presence of the fibers, it was not possible to precisely determine the mass of the matrix inside the samples, therefore the comparison with the DSC carried out on the PEKK, showed in Fig. 20, can only be qualitative.

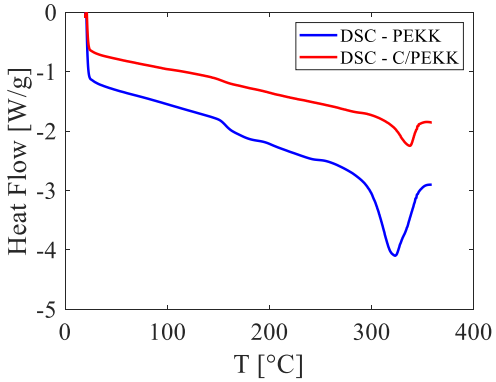

Fig. 20 Comparison between heat flow vs T curves of PEKK and C/PEKK

The C/PEKK either shows no presence of the exothermic peak, meaning that the matrix, like the polymer, does not increases its crystalline percentage only because of thermal load. The C/PEKK heat flow vs temperature curves during 1st heating, shows difference values of T_g and melting peak values, but a globally similar trend compared to PEKK.

3.4 Employment of a semi-analytical homogenization-localization method for the interpretation of test results

The composite experimental tensile test curves was reconstructed starting from the polymer experimental data only, through a homogenization-localization method.

A first guess set of polymer properties (P0) is introduced to evaluate the ply properties employing Tsai-Hill micromechanics equations (Halpin and Tsai 1967). The composite properties are calculated through Herakovich's lamination theory (Herakovich 1998), and, once the composite stress is introduced, it is possible to calculate the composite strain. Going downward it is also possible to calculate the ply stress and strain fields.

Freour's localization method (Fréour *et al.* 2005) is then employed: this method is the adaptation of the Mori-Tanaka self-consisted method (Mori and Tanaka 1973) to the case of the composite, where the ellipsoidal inclusion inside the matrix are replaced by infinite cylinders. The ply strain and properties, along the polymer properties, inserted in the localization method allow to evaluate the matrix stress and strain fields.

Since both methods were developed for the linear elastic case, to describe the non-linearity of the tensile tests, matrix properties are allowed to vary according to the composite stress. At the end of the 1st step of calculation, the matrix stresses result function of the polymer properties and of the composite stress ($\bar{\bar{\sigma}}_m = f\left(P_0, \bar{\bar{\sigma}}_c(j)\right)$. The matrix equivalent von Mises stress is compared to the polymer equivalent von Mises stress, the latter corresponding to a specific set of polymer of properties ($\sigma_m^{VM}\left(P_0, \bar{\bar{\sigma}}_c(j)\right) = \sigma_{resin}^{VM}(P_1)$, exploiting the bijective relation between stress, strain and properties of the tensile test. The set of properties P1 is then compared to P0 and if the difference is below a threshold, all the stress and strain fields calculated are validated, otherwise they are recalculated with the new set of polymer properties P1, and the loop continues until convergence is reached. The whole procedure is then repeated for each experimental composite stress. To whole algorithm is resumed in Fig. 21.

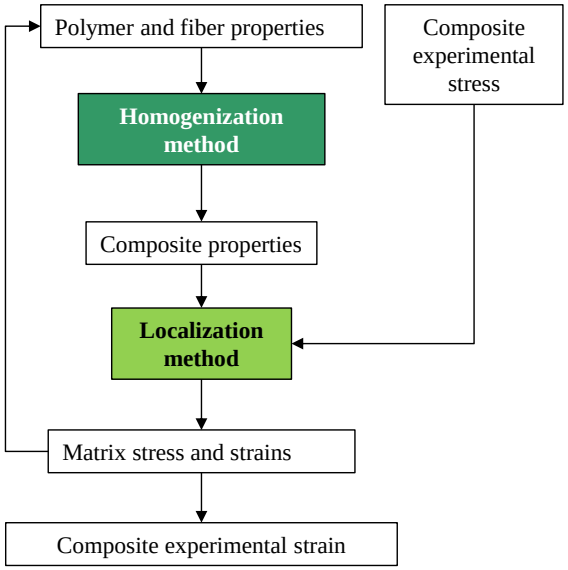

Fig. 21 Algorithm of the homogenization /localization method

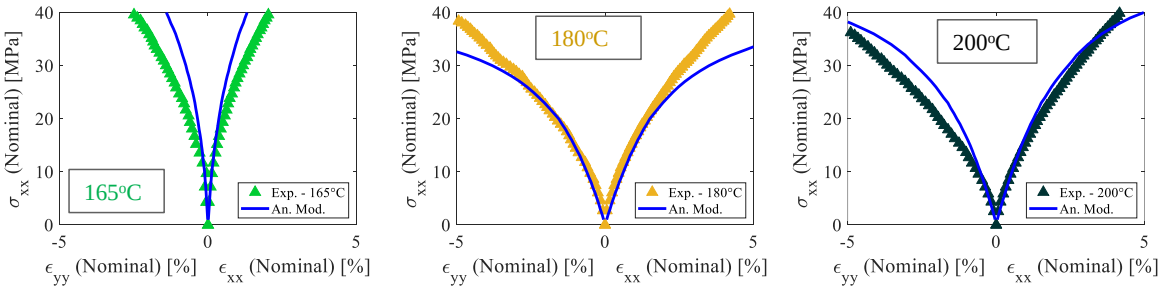

Fig. 22 Comparison between experimental tensile test on C/PEKK and the analytical method at 165℃, 180℃ and 200℃

Fig. 22 shows the reconstruction of the tensile test curves at 1 mm/min and at 165°C, 180°C and 200°C: the model is capable of describing the initial part of the curves, diverging rapidly at higher strains: this seems to confirm the fact that only the initial part of the composite tensile test curve is matrix dominated and that the matrix behavior inside the composite is similar to that of the polymer.

4. Conclusions

DMA, tensile and DSC tests are carried out on SC 7002 PEKK polymer and [(±45)2, +45]s C/PEKK composite samples, in order to characterize their mechanical behavior below and above Tg, particularly between Tg and 200°C.

DMA and tensile tests on PEKK samples show that there is a loss of more than 90% of the mechanical properties when the temperature is increased above T_g. Moreover, the material becomes lesser sensitive to temperature and time effects as the temperature is raised above T_g.

DSC tests show that there are no morphological changes in the analyzed temperature range due to thermal-mechanical loads.

DMA and tensile tests on C/PEKK samples show that there is a loss of more than 80% of the mechanical properties when the temperature is increased over T_g. All the tests show that the behavior of C/PEKK samples is similar to that of the PEKK pure polymer, at least in the low strain region. A homogenization-localization analytical method is employed to describe the mechanical behavior of the C/PEKK over this region, by employing as an input the properties of the PEKK pure polymer properties.

Acknowledgments

This work pertains to the French government program "IMPEKKABLE" (reference ANR-15-CE08-0016) which aims to employ PolyEtherKetoneKetone (PEKK) as carbon fiber reinforced matrix to replace metallic components in the aircraft pylons. Thus, the aim of the project is therefore to define the Material Operating Limit and to simulate the operating conditions.

The ANR program "IMPEKKABLE" is in collaboration with AIRBUS GROUP SAS Département Innovations, ARKEMA France, Ecole Nationale Supérieure d'Arts et Métiers - Laboratoire de Procédés et Ingénierie en Mécanique et Matériaux. Thanks to Airbus SAS and especially to Dr. A. Vinet for the tensile tests on the C/PEKK at $T< T_g$. Thanks to other participants at the IMPEKKABLE project for Pprime : S. Castagnet, O. Smerdova, M.C. Lafarie. Thanks also to: F. Foti, V. Caccuri, M. Morriset, D. Mellier, J. Lefort and the whole équipe technique.

References

Biron, M. (2018), *Chapter 9 - Future Prospects for Thermoplastics and Thermoplastic Composites*, in *Thermoplastics and Thermoplastic Composites (Third Edition)*, William Andrew Publishing, Norwich, New York, U.S.A.

Brinson, L.C. and Gates, T.S. (1995), "Effects of physical aging on long term creep of polymers and polymer matrix composites", *Int. J. Solids Struct.*, **32**(6/7), 827-846. https://doi.org/10.1016/0020-7683(94)00163-Q.

Chelaghma, S., De Almeida, O., Marguerès, P., Passieux, J.C., Péric, J.N., Vinet, A. and Reine, B. (2017), "Investigation of PEKK crystal morphology and modelling of the crystallization kinetic of PEKK composites", *Proceedings of the 20th Journées Nationales sur les Composites*, Paris, France, June.

Choupin, T., Fayolle, B., Régnier, G., Paris, C., Cinquin, J. and Brulé, B. (2017), "Isothermal crystallization kinetic modeling of poly(etherketoneketone) (PEKK) copolymer", *Polymer*, **111**, 73-82. https://doi.org/10.1016/j.polymer.2017.01.033.

Fréour, S., Jacquemin, F. and Guillen, R. (2005), "On an analytical Self-Consistent model for internal stress prediction in fiber-reinforced composites submitted to hygroelastic load", *J. Reinf. Plast. Compos.*, **24**, 1365-1377. https://doi.org/10.1177/0731684405049887.

Gabrion, X., Placet, V., Trivaudey, F. and Boubakar, L. (2016), "About the thermomechanical behaviour of a carbon fibre reinforced high-temperature thermoplastic composite", *Compos. Part B Eng.*, **95**, 386-394. https://doi.org/10.1016/j.compositesb.2016.03.068.

Guo, Y. and Bradshaw, R.D. (2007), "Isothermal physical aging characterization of Polyether-ether-ketone (PEEK) and Polyphenylene sulfide (PPS) films by creep and stress relaxation.", *Mech. Time-Depend. Mater.*, **11**(1), 61-89. https://doi.org/10.1007/s11043-007-9032-7.

Gurtin, M.E., Fried, E. and Anand, L. (2010), *The Mechanics and Thermodynamics of Continua*, Cambridge

University Press, Cambridge, U.K.
Halpin, J.C. and Tsai, S.W. (1967), "Environmental factors in composite design", Air Force Materials Laboratory Technical Report, AFML-TR-67-423.
Herakovich, C.T. (1998), *Mechanics of Fibrous Composites*, John Wiley and Sons Inc., New York, U.S.A.
Li, C. and Strachan, A. (2019), "Prediction of PEKK properties related to crystallization by molecular dynamics simulations with a united-atom model", *Polymer*, **174**, 25-32. https://doi.org/10.1016/j.polymer.2019.04.053.
Martín, M.I., Rodríguez-Lence, F., Güemes, A., Fernández-López, A., Pérez-Maqueda, L.A. and Perejón, A. (2018), "On the determination of thermal degradation effects and detection techniques for thermoplastic composites obtained by automatic lamination", *Compos. Part A Appl. Sci. Manufact.*, **111**, 23-32. https://doi.org/10.1016/j.compositesa.2018.05.006.
Martineau, L., Chabert, F., Bernhart, G. and Djilali, T. (2016), "Mechanical behavior of amorphous PEEK in the rubbery state", *Proceedings of the ECCM17 - 17th European Conference on Composite Materials*, Munich, Germany, June.
Mori, T. and Tanaka, K. (1973), "Average stress in matrix and average elastic energy of metals with misfitting inclusion", *Acta Metallurgica*, **21**, 571-574. https://doi.org/10.1016/0001-6160(73)90064-3.
Oliver, W.C. and Phar, G.M. (1992), "An improved technique for determining hardness and elastic modulus using load and displacement sensing indentation experiments", *J. Mater. Res.*, **7**(6), 1564-1583. https://doi.org/10.1557/JMR.1992.1564.
Pappadà, S., Salomi, A., Montanaro, J., Passaro, A., Caruso, A. and Maffezzoli, A. (2015), "Fabrication of a thermoplastic matrix composite stiffened panel by induction welding", *Aerosp. Sci. Technol.*, **43**, 314-320. https://doi.org/10.1016/j.ast.2015.03.013.
Sun, C.T., Chung, I. and Chang, I.Y. (1992), "Modeling of elastic-plastic behavior of LDF™ and continuous fiber reinforced AS-4/PEKK composite", *Compos. Sci. Technol.*, **43**(4), 339-345. https://doi.org/10.1016/0266-3538(92)90057-A.
Sutton, M.A., Orteu, J.J. and Schreier, H.W. (2009), *Image Correlation for Shape, Motion and Deformation Measurements. Basic Concepts, Theory and Applications*, Springer, New York, U.S.A.
Tadini, P., Grange, N., Chetehouna, K., Gascoin, N., Senave, S. and Reynaud, I. (2017), "Thermal degradation analysis of innovative PEKK-based carbon composites for high-temperature aeronautical components", *Aerosp. Sci. Technol.*, **65**, 106-116. https://doi.org/10.1016/j.ast.2017.02.011.
Vinet, A., Fayolle, A., Gigliotti, M. and Brulé, B. (2019), "Comportement des matrices PEKK en oxydation", *Proceedings of the 21st Journées Nationales sur les Composites*, Bordeaux, France, July.

EC